VNet: An End-to-End Fully Convolutional Neural Network for Road Extraction From High-Resolution Remote Sensing Data

ABOLFAZL ABDOLLAHI[1], BISWAJEET PRADHAN[1,2,3], (Senior Member, IEEE), AND ABDULLAH ALAMRI[4]

[1]Centre for Advanced Modelling and Geospatial Information Systems (CAMGIS), Faculty of Engineering and IT, University of Technology Sydney, Sydney, NSW 2007, Australia
[2]Department of Energy and Mineral Resources Engineering, Sejong University, Seoul 05006, South Korea
[3]Earth Observation Center, Institute of Climate Change, Universiti Kebangsaan Malaysia, Bangi 43600, Malaysia
[4]Department of Geology and Geophysics, College of Science, King Saud University, Riyadh 11451, Saudi Arabia

Corresponding author: Biswajeet Pradhan (biswajeet.pradhan@uts.edu.au)

ABSTRACT One of the most important tasks in the advanced transportation systems is road extraction. Extracting road region from high-resolution remote sensing imagery is challenging due to complicated background such as buildings, trees shadows, pedestrians and vehicles and rural road networks that have heterogeneous forms with low interclass and high intraclass differences. Recently, deep learning-based techniques have presented a notable enhancement in the image segmentation results, however, most of them still cannot preserve boundary information and obtain high-resolution road segmentation map when processing the remote sensing imagery. In the present study, we introduce a new deep learning-based convolutional network called VNet model to produce a high-resolution road segmentation map. Moreover, a new dual loss function called cross-entropy-dice-loss (CEDL) is defined that synthesize cross-entropy (CE) and dice loss (DL) and consider both local information (CE) and global information (DL) to decrease the class imbalance influence and improve the road extraction results. The proposed VNet+CEDL model is implemented on two various road datasets called Massachusetts and Ottawa datasets. The suggested VNet+CEDL approach achieved an average F1 accuracy of 90.64% for Massachusetts dataset and 92.41% for Ottawa dataset. When compared to other state-of-the-art deep learning-based frameworks like FCN, Segnet and Unet, the proposed approach could improve the results to 1.09%, 2.45% and 0.39%, for Massachusetts dataset and 7.21%, 1.86% and 2.68%, for Ottawa dataset. Also, we compared the proposed method with the state-of-the-art road extraction techniques, and the results proved that the proposed technique outperformed other deep learning-based techniques in road extraction.

INDEX TERMS CEDL, road extraction, remote sensing, VNet network.

I. INTRODUCTION

High-resolution remote sensing images has been utilized in varieties of applications; building footprint extraction [1], urban area planning [2], disaster management [3] and many others. One of the main features in the urban regions is the road network, which plays a principal role in the transportation systems development such as planning of urban

The associate editor coordinating the review of this manuscript and approving it for publication was Wenming Cao.

areas, unmanned vehicles and automatic road navigation as well [4]. In the remote sensing image processing field, road network extraction has become one of the key topics for researchers [5]–[7], and high-resolution remote sensing data has become a primary source of data for updating road network database in real-time [8]. Thus, introducing a novel robust approach for road network extraction from these images would be useful for intelligent transportation systems (ITS) and geospatial information systems (GIS) [9]. However, there are some issues that make the process of

extracting road part from high-resolution remote sensing imagery more difficult. For example, high-resolution images are complex and other features such as vehicles on the roads, building on the roadsides and trees shadows can be observed from these images. This is because these features present similar spectral values as road pixel values and inadequate context of road parts is similar with these objects in the remote sensing imagery [10]. In addition, road segments are irregular and road networks present complex structure in the remote sensing images [11].

To the best of our knowledge, traditional techniques are time consuming and include numerous errors caused by human operators [12]. In recent years, researchers have proposed various kinds of approaches for road extraction from remote sensing images that include supervised [13] and unsupervised classification techniques [14]. These techniques generally utilize textural, photometric, and geometric characteristics to extract road parts, and they are based on image classification. Unsupervised approaches normally utilize clustering methods to extract road class from remote sensing images. Unsalan and Sirmacek [15] used graph theory to extract road networks from Aerial, QuickBird, IKONOS and Geoeye images. The achieved results illustrated that the proposed method is reliable for road extraction on such imagery. Khesali *et al.* [16] combined TerraSAR-X with high-resolution IKONOS images to segment road networks. They first implemented neural network based on different spectral and textural information to detect road parts. Next, they used knowledge-based fusion approach to extract road from the images. The obtained results indicated that the proposed method can be applied in extracting road network in a reliable meaner. Miao *et al.* [17] extracted primary points from the road seed points from the aerial imagery with a spatial resolution of 0.3 meter based on the mean shift method that is a semi-automatic technique. Then, for separating non-road and road class, they used a threshold. In contrast, supervised methods including deep learning techniques [6], [18], [19], random decision forest (RF) [20] and support vector machine method (SVM) [21] use labeled samples for extracting roads and they showed better results compared with the unsupervised approaches. Da-Ming *et al.* [22] implemented a hybrid method of Fuzzy C-mean and SVM for image segmentation and then applied Markov Random Filed (MRF) for road extraction from Google imagery. Anwer *et al.* [23] classified remote sensing scenes based on the two-stream deep learning framework that fused RGB stream and texture coded mapped imagery. In another work, Simler [24] proposed SVM technique to exploit both spectral and spatial characteristics and then extracted road class from aerial imagery with spatial resolution of 0.5 meter. Yager and Sowmya [25] applied SVM method for road extraction from aerial imagery with spatial resolution of 0.45 meter based on some important features such as edge length, intensity and gradient. Although all the mentioned techniques achieved reliable accuracy for road extraction from high-resolution remote sensing imagery, they missed some road segments

where there is low visibility of road segments in the images. Also, the proposed techniques faced some errors in road segmentation because of the road-like patterns in some areas of images.

The artificial intelligence (AI) approaches have now appealed the attention of scholars for road networks extraction from high-resolution remote sensing imagery encouraged by the reliable efficiency of deep convolutional neural architectures in various types of applications [26]–[30]. Wang *et al.* [9] extracted road class from high-resolution aerial and Google Earth imagery on the basis of finite state machine (FSM) and deep neural network (DNN). The proposed method includes two major steps for extracting road class called training and tracking steps. They showed that the proposed approach could not achieve a reliable result for road extraction from complicated images that road is surrounded by other occlusions. A convolutional neural network (CNN) was proposed by [31] for road extraction from Geoeye satellite imagery and Pleiades-1A satellite images with 0.5 spatial resolution. They also used line integral approach to connect small gaps and preserve edge information. However, the proposed method did not yield accurate results for quality and completeness metrics owing to the texture complexity of different objects in the images. A deep encoder-decoder network (DCED) was implemented by [32] for road extraction from Massachusetts road images. They applied landscape metrics approach to remove non-road pixels, data augmentation method like rotating the images to increase the number of training images, and Exponential Linear Unit (ELU) activation function against rectified linear unit (RELU) function to improve the output accuracy. They proved that the suggested method outperformed other comparison methods in road extraction. In another work, [33] used deep CNN model called SegNet to extract road class from Thailand Earth Observation System (THEOS) images and Massachusetts road images. In addition to using ELU function and landscape metrics, they applied conditional random field (CRF) at the last step for the segmented road map sharpening. The results showed that the proposed method could not obtain accurate segmentation map for THEOS images compared to Massachusetts images.

A new deep framework based on cascading end-to-end network (CasNet) was performed by [10] to extract road networks from Google Earth imagery. Some data augmentation techniques and regularization approach were applied to reduce over-fitting. They illustrated that the proposed model was efficient in road extraction from non-complex areas where other obstacles do not cover the road networks. Varia *et al.* [34] extracted road networks from unmanned aerial vehicle (UAV) images based on fully convolutional network (FCN) and generative adversarial network (GAN). Although the results confirmed that the methods were effective in road extraction, the proposed approaches misclassified non-road pixels as road pixels in complex areas that lead to predicting more false positive (FP) pixels. Xu *et al.* [35] implemented a deep residual framework called M-Res-Unet

model combined with a pre-processing technique named Gaussian filter for road semantic segmentation from World-View2 satellite imagery. The proposed method however could not perform well in road extraction from areas in the images where the other objects present similar spatial and color distribution as road object. A new framework on the basis of FCN architecture called U-shaped FCN (UFCN) was introduced by [19] for road segmentation from UAV images. For increasing the size of dataset, some augmentation methods were applied. The suggested model compared with other approaches such as SVM, one-dimensional CNN (1D-CNN) and two-dimensional (2D-CNN) and results indicated that the proposed technique surpassed other comparison methods in road extraction. Buslaev *et al.* [18] extracted road networks from Digital Globe's satellite imagery with spatial resolution of 50 cm based on Unet architecture. They used data augmentation approaches and produced a loss function that considers Intersection Over Union (IOU) and binary cross entropy concurrently to improve the output results. They achieved an accuracy of 64% for IOU indicating that the proposed technique was not that effective in road extraction. Also, a deep residual network based on Unet model was introduced by [5] for road networks segmentation from Massachusetts images. They used residual units and skip connections inside the model to streamline the model training and build a network with fewer parameters, respectively. The proposed technique was compared with other state-of-the-art approaches that showed better results in road extraction than others. However, the suggested technique was not effective in accurate road segmentation from areas where the road networks are covered by trees and parking lots.

Thus, in this research, we used a novel deep learning-based convolutional network called VNet model with 2D convolutional kernel to extract road networks from two different high-resolution remote sensing imagery such as Massachusetts road dataset (Aerial images) and Ottawa road dataset (Google Earth images) and produced a high-resolution segmentation output. As far as we know, the proposed method has not been used in the literature and this is for the first time this kind of approach has been proposed for the given task. The proposed method trained end-to-end and leverage the power of fully convolutional neural networks to process high-resolution remote sensing imagery. In the suggested VNet network, pooling layers were replaced with convolutional layers that resulted in a shorter memory footprint throughout the training process. Also, a new objective loss function on the basis of cross entropy and dice loss (CEDL) was used to (i) combine local information (CE) and global information (DL), (ii) diminish the influence of class imbalance, and (iii) improve the road segmentation results. In addition, a new non-linearities activation function named parametric rectified linear unit (PRelu) was applied rather than rectified linear unit (ReLU) function to enhance accuracy at a negligible additional computational cost and its performance is better than ReLU for large-scale data processing. The remnant of the manuscript is designed

as follows: the overall methodology of the suggested VNet architecture is presented in Section II. Section III illustrates the dataset preparation, evaluation metrics and extramental results achieved by the proposed technique. Section IV indicates the comparison results for the proposed network and other state-of-the-art deep learning-based networks. Lastly, Section V highlights the conclusion.

II. METHODOLOGY

The overall methodology of the suggested VNet-based method for road extraction from high-resolution remote sensing imagery is shown in Figure 1. At the first step, two different road datasets called Massachusetts and Ottawa are used to prepare the training, validation and test images for training and evaluating the proposed method. Then, the architecture of the proposed VNet approach along with the new CEDL function is defined. Following this, the training samples are used to train the VNet model and then test images are used to extract road networks and evaluate the performance of proposed methods.
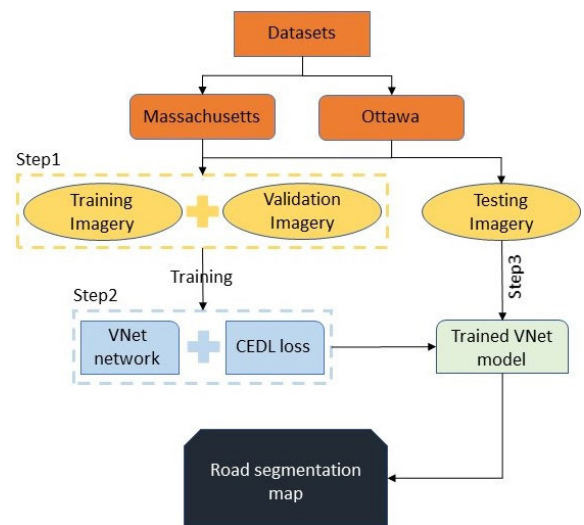

FIGURE 1. The overall framework of the proposed VNet network for road extraction.

A. VNet ARCHITECTURE

A schematic presentation of the proposed VNet model is shown in Figure 2. The proposed VNet approach is comprised of two main parts: the left section that includes a compression path and the right part that decompresses the input till its initial size is attained. Convolutions with appropriate padding are all performed, aiming to both exploit features from the input and decrease its resolution using proper stride at the end of each stage.

The architecture of the proposed VNet network is similar to the widely used Unet [36] model, but with some differences. The left part of the VNet architecture is split into various phases operating at different resolutions. One to three convolution layers exist in each stage. A residual function can
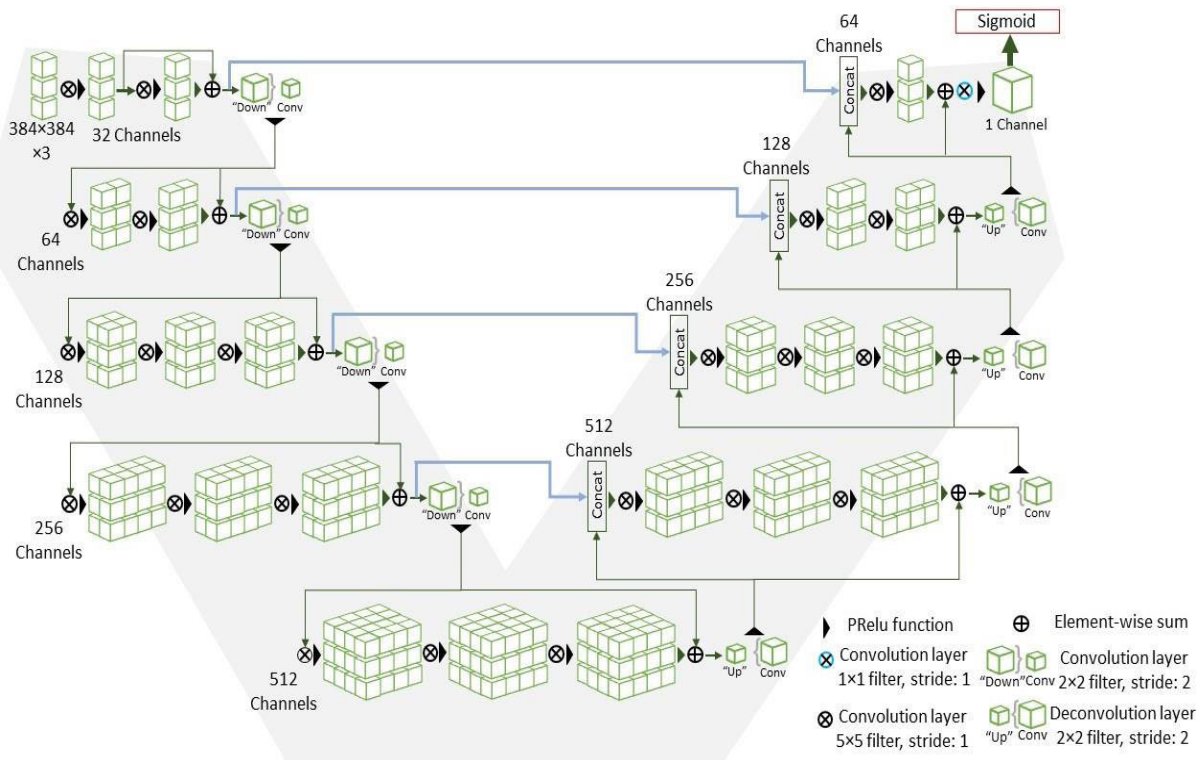
FIGURE 2. The architecture of VNet network including two mains expansive (right side) and contracting parts (left side).

be learned in each phase as we formulate each stage similar to the method illustrated in [37]. In other words, in order to enable learning a residual function, the input of every phase is processed through the non-linearities and utilized in the convolution layers and then appended to the output of the final convolution layer of that phase. This network guarantees convergence in comparison with non-residual learning architecture such as Unet. Also, in each stage, the convolutional layers with the size of 5×5 is performed. The convolution process is expressed using Equation (1).

$$
\begin{aligned}
&x_k(ii, jj) \\
&= \sum_{n=1}^{N} \left\{ \sum_{p=0}^{W_f-1} \sum_{q=0}^{h_f-1} x_n(i \cdot s_f + p, j \cdot s_f + q) \cdot h_k(p, q) \right\} + b_k
\end{aligned}
\tag{1}
$$

where b_k is the bias parameter of the k-th filter that is shared among all locations (p,q), s_f is the sampling stride, h_k(p,q) is the weight value at (p,q) of the k-th filter, x_k(ii,jj) is the pixel value at (ii,jj) in the k-th filter size of the input map, and x_n(ii,jj) is the pixel value at (ii,jj) in the n-th channel of an input feature map.

The resolution of data is reduced as it proceeds through various phases along the compression path and this is implemented using convolutional layer with size of 2×2 and stride 2. The size of the resulting feature maps is halved as the second operation considers only non-overlapping 2×2 patches and extract features [38]. We replaced max-pooling layers with convolutional layers in our method that serves as

the same objective as pooling layers incited by [38]. We used these convolutional operations for doubling the number of feature maps. This is due to the formulation of the method as a residual framework, and since the number of feature channels double at every phase of the VNet compression path. Using convolutional layers instead of pooling layers results to the network to have a smaller memory footprint throughout the training. Pooling operation did down-sampling the features, but we wanted to keep all the features as possible. Therefore, the advantages of using convolutional layers rather than pooling layers in our proposed method is that to process inputs in higher resolution and detect fine-details as well as capture more contextual information by broadening the view of input data [39]. Decreasing the size of input and increasing the receptive field of the features being assessed in the following layers of network is operated by down-sampling step. In the left section of the network, the number of features that are assessed by each phase is two times higher than one of the prior layer. For activation function (Equation 2), there are several functions such as tanh, rectified function and so on that can be used.

$$
Z(x_k(ii, jj)) = f\left(\sum_{k=1}^{k} x_k(ii, jj) \cdot w_k + b_k\right) \Leftrightarrow Z = f(X \cdot W + b)
\tag{2}
$$

where w is a weight vector, b is a bias vector, and x_k(ii,jj) is used as input to the activation function of the neural network that is the output of convolution operation.

In this work, a non-linearity function called PRelu (Equation 3) proposed by [40] is implemented throughout the model. PRelu function can be optimized concurrently with other layers and can be trained using back-propagation. This function enhances accuracy at a negligible additional computational cost, and adaptively learns the parameters of the rectifiers. For the large-scale image classification, the authors reported that its performance is better than ReLU function.

$$y_i = \begin{cases} x_i & if \ x_i \geq 0 \\ \dfrac{x_i}{a_i} & if \ x_i \leq 0, \end{cases} \quad (3)$$

where a_i defines as a fixed parameter in the range of $(1, +\infty)$ and it is learned via back-propagation in the training.

In order to assemble and gather the essential information to output of two channels segmentation map, the right part of the network expands the spatial support of the lower resolution feature maps and extract features. The last convolutional layer with the kernel size of 1×1 produces the output with a similar size of the input data and computes the two features maps. Also, we used sigmoid function in this layer that converts these two feature maps into probabilistic segmentation maps of the background and foreground areas. Compared to the Unet architecture, after every phase of the right part of the network, a deconvolutional operation was followed by one to three convolution layers. This includes half the number of 5×5 kernels that were applied in the past layer and was used to increase the size of input. We also resorted to learn residual functions in the convolutional phases of the right part of the network similar to the left portion. Next, the extracted features were forwarded from early phases of the left portion of the network to the right section similar to [36] that is shown in Figure 2 by horizontal links. Subsequently, we improved the quality of last contour prediction in this way by gathering fine-grained details that would have been otherwise missed during the compression stage. It is also observed that the convergence time of the model has been improved by these connections.

B. LOSS FUNCTION

In feature semantic segmentation from high-resolution remote sensing images such as road networks segmentation, it is common that road pixels occupy just a pretty tiny area of the image. This usually can be the cause of confining learning process in the regional minima of the loss function, generating a model whose anticipations are heavily prejudiced to the background. Therefore, the foreground area is usually only partly identified or even missed. To tackle this problem, multiple prior methods on the basis of re-weighting the samples where background areas are assigned less significance than foreground areas ones through learning such as weighted cross-entropy [41] and dice loss [42] have been presented. Equation 4 defines the dice loss (DL) between two binary

classes whose values are ranging between 0 and 1.

$$DL = \dfrac{2 \sum\limits_{i}^{N} p_i g_i}{\sum\limits_{i}^{N} p_i^2 + \sum\limits_{i}^{N} g_i^2} \quad (4)$$

where $g_i \in G$ is the ground truth pixels, $p_i \in P$ is the predicted binary pixels and N defines as total pixels. The dice formulation can be modified with producing the gradient measured regarding the j-th pixels of the anticipation (Equation 5). As a result, for establishing the right balance between background pixels and foreground ones, we do not require to allocate weights to the various classes samples using this formulation.

$$\dfrac{\partial D}{\partial p_j} = 2 \left[\dfrac{g_j(\sum\limits_{i}^{N} p_i^2 + \sum\limits_{i}^{N} g_i^2) - 2p_j(\sum\limits_{i}^{N} p_i g_i)}{(\sum\limits_{i}^{N} p_i^2 + \sum\limits_{i}^{N} g_i^2)^2} \right] \quad (5)$$

In this study, since we have the same issue of imbalance classes such as road pixels (foreground) and non-road pixels (background) we introduced a new dual objective loss function (CEDL) that incorporates both cross-entropy loss function (CE) and dice coefficient (DL) to reduce the influence of class imbalance issues. Equation 6 defines the new loss function (L) that is a mixture of CE and DL. Note that DL returns a scalar while CE returns a tensor of every image in the batch. In other words, we mixed global information (DL) and local information (CE) to extract road network more accurately.

$$CEDL = CE(p_i, g_i) + DL(p_i, g_i) \quad (6)$$

III. RESULTS

In this section, first, the different high-resolution remote sensing road datasets named Massachusetts and Ottawa were highlighted. Then, the measurement factors that were used to evaluate the performance of the proposed VNet network for road extraction are explained. Finally, the experimental results achieved by the suggested approach based on three different loss functions called Cross entropy (CE), Dice Loss (DL) and CEDL are discussed and compared.

A. DATASETS

1) MASSACHUSETTS ROAD DATASET

This dataset [43] contains 1171 aerial imagery with the primary spatial resolution of 0.5 m and dimension of 1500×1500. Due to computational restrictions, we split the main images into smaller parts with the size of 384×384 that include good quality and complete information. The dataset that we used for validating the proposed method for road extraction includes 4135 images that we divided it into 215 images for test, 120 images for validation and 3800 images for training. For expanding the dataset, some data augmentation methods such as vertical flip, rotation and horizontal flip are also used. Moreover, for overcoming

the over-fitting issue, we added a dropout of 0.5 to deeper convolutional layers. Some examples in the Massachusetts road dataset is illustrated in Figure 3.

FIGURE 3. Some sample imagery in Massachusetts road dataset. The main imagery and corresponding ground truth maps are illustrated in the first and second columns, respectively.

FIGURE 4. Some sample imagery in Ottawa road dataset. The main imagery and corresponding ground truth maps are illustrated in the first and second columns, respectively.

2) OTTAWA ROAD DATASET

This dataset includes Google Earth images with spatial resolution of 0.21 m that encompasses 21 typical urban regions covering about 8 km^2 of Ottawa, Canada [44]. The road labels were annotated manually and compared to other datasets such as [43], [45] and [10]. This dataset is more challenging and comprehensive as it covers different urban areas with different complexity. In this study, we divided the dataset into images with a size of 384×384 to validate the proposed method. The final dataset contained 1005 images that were split into 899 training images, 62 validation images and 44 test images. Also, we used data augmentation techniques like flipping horizontally and vertically and rotating the images to expand the dataset. Some examples in the Ottawa road dataset is depicted in Figure 4. The whole process of applying the proposed model for road network extraction from high-resolution remote sensing imagery is functioned
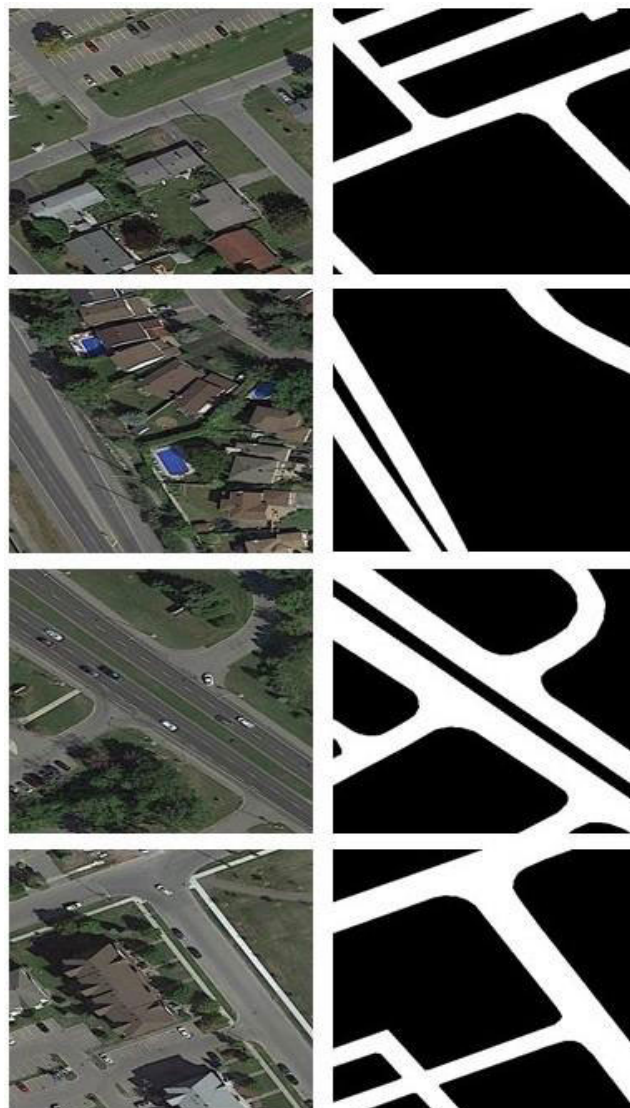
on a GPU Nvidia Quadro RTX 6000 with a computation capacity of 7.5 and a memory of 24 GB under the framework of Keras with Tensorflow backend.

B. PERFORMANCE MEASUREMENT FACTORS

We applied three main measurement factors such as F1, Matthew correlation coefficient (MCC) and Intersection over union (IOU) to assess the accuracy of the introduced VNet network for road extraction from Massachusetts and Ottawa road datasets. MCC (7) defines as a correlation coefficient between identified binary classification and predicted classification that provide a value between -1 and $+1$.

$$MCC = \frac{TP.TN - FP.FN}{\sqrt{(TP + FP)(TP + FN)(TN + FP)(TN + FN)}} \quad (7)$$
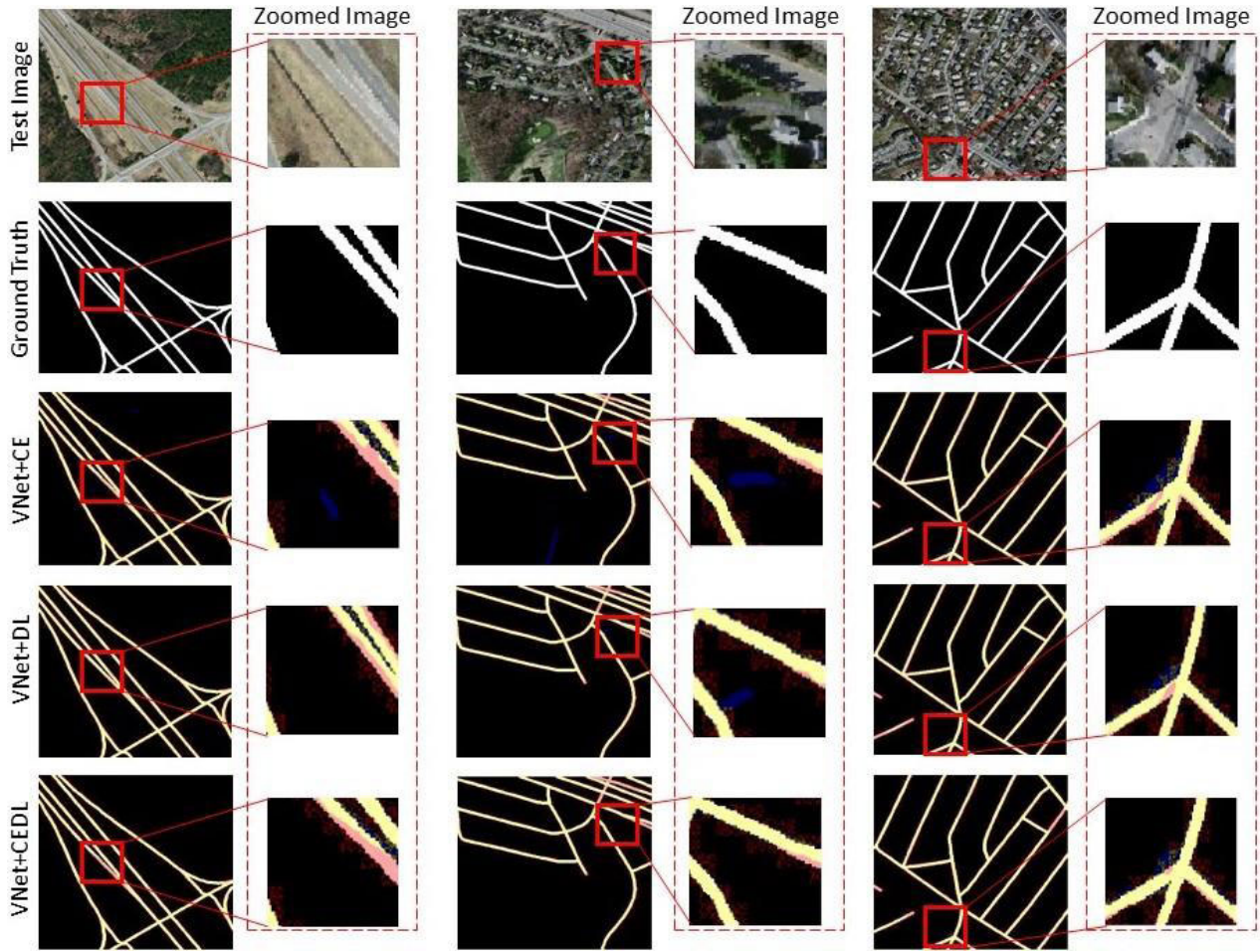
FIGURE 5. The achieved outcomes using the proposed VNet+CE, VNet+DL and VNet+CEDL from Massachusetts road dataset. The second, fourth and sixth columns present the zoomed outcomes of the prior column. The black, yellow, blue, and red colors show the TNs, TPs, FPs, and FNs, respectively.

IOU (8) indicates the number of pixels that are common between the predicted and target masks divided by the whole amount of available pixels over both masks.

$$IOU = \frac{TP}{TP + FP + FN} \qquad (8)$$

Finally, F1 (9) is defined as a mixture of precision and recall metrics [46], [47].

$$F1 = \frac{2 \times \mathrm{Pr}ecision \times \mathrm{Re}call}{\mathrm{Pr}ecision + \mathrm{Re}call} \qquad (9)$$

C. EXPERIMENTAL RESULT

These days, access to very high-resolution satellite data has become easier than ever. On the other hand, road network in the urban areas are one of the most significant ones that plays a vital task in various applications of Geospatial Information System (GIS) like urban planning, traffic managing and navigation systems [11]. Moreover, extracting road networks from high-resolution remote sensing imagery and updating road database is very beneficial for urban management. As a result, in this work, we implemented a new

deep learning-based VNet architecture to segment road parts from two different remote sensing datasets. In this section, the results achieved by the proposed approach based on CE, DL and CEDL loss functions are highlighted. Figure 5 and Figure 6 illustrate the obtained results via the suggested technique based on CE loss function, DL and CEDL for Massachusetts road dataset and Ottawa dataset, respectively. The figures are represented in six columns and five rows. The main RGB images, the ground truth labels, the results achieved by the VNet+CE, VNet+DL and VNet+CEDL are presented in the first, second, third, fourth and last row, respectively. Also, the second, fourth and sixth columns show the zoomed outcomes. Based on the figures, the suggested VNet network with all loss functions could generally segment road class from high-resolution remote sensing data precisely. However, the results achieved by VNet+CEDL is more accurate than VNet+CE and VNet+DL. In fact, VNet+CE and VNet+DL predicted more false positive pixels (FPs) (shown as blue pixels) and less false negative pixels (FNs) (shown as red pixels) in the both datasets that lead to achieving lower accuracy compare to VNet+CEDL for road extraction.
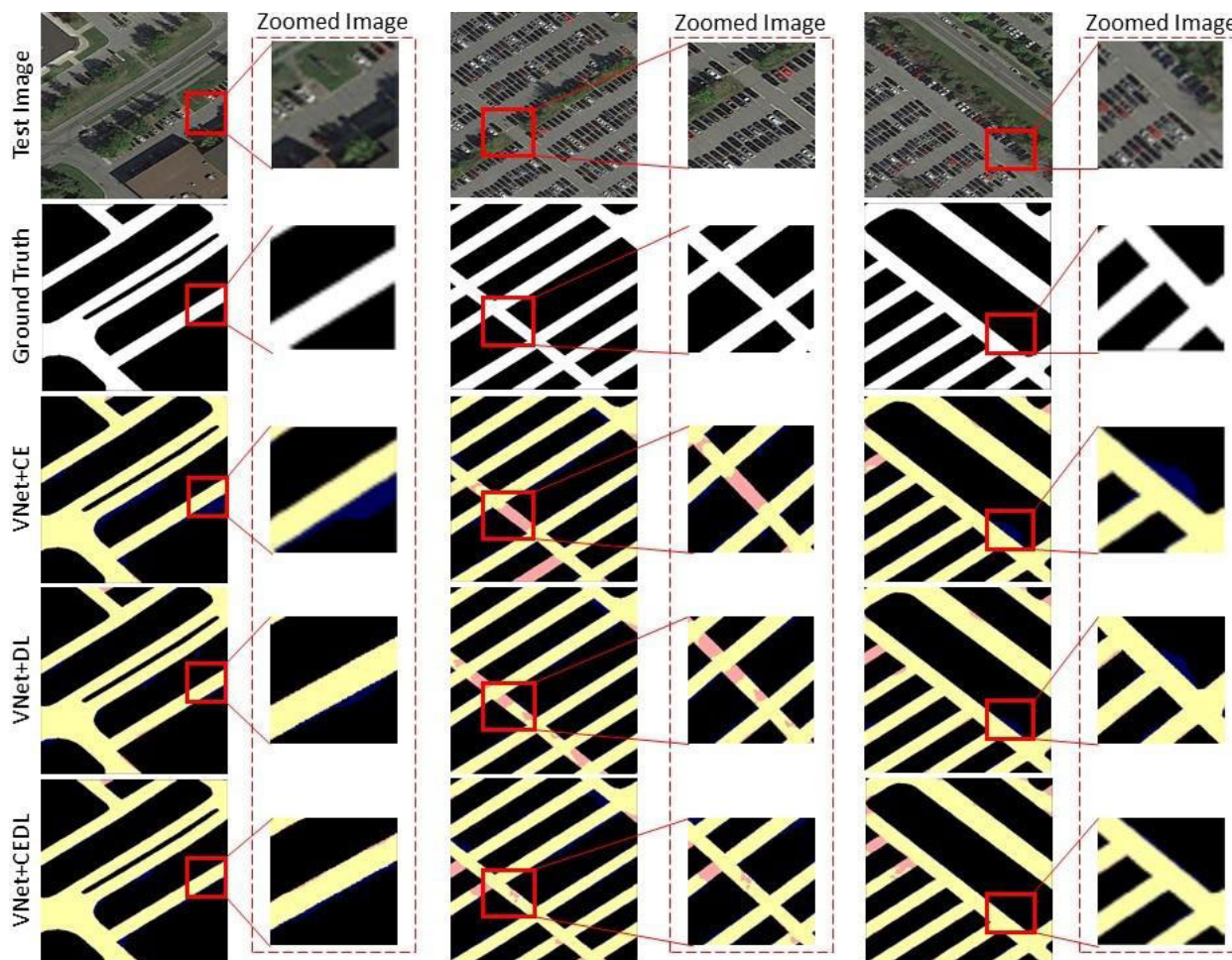
FIGURE 6. The achieved outcomes using the suggested VNet+CE, VNet+DL and VNet+CEDL from Ottawa road dataset. The second, fourth and sixth columns present the zoomed outcomes of the prior column. The black, yellow, blue, and red colors show the TNs, TPs, FPs, and FNs, respectively.

The proposed VNet+CE and VNet+DL models could not segment road part from remote sensing data where the road network is covered by shadows or in the junction parts. Therefore, by using new CEDL loss function that consider both local and global information and solve the issue of lessening the influence of class imbalance, the proposed VNet plus CEDL could improve the results.

Moreover, we assessed the accuracy measurements of VNet+CE, VNet+DL, and VNet+CEDL for Massachusetts and Ottawa datasets to probe the capability of the proposed network for road extraction. Table 1 and Table 2 depict the accuracy of each defined metric for the Massachusetts and Ottawa road datasets, respectively. As it can be seen from both Tables, the proposed VNet+CEDL model could achieve higher average accuracy than VNet+CE and VNet_DL for F1, MCC and IOU with 90.11%, 88.30% and 82.07%, respectively for Massachusetts dataset; and 93.54%, 89.89% and 87.93%, respectively for Ottawa dataset. Note that the proposed VNet+CEDL network achieves good results for the road segmentation from both datasets and determines that the segmented road sections are close to labels,

TABLE 1. Comparing VNet model with CE, DL and CEDL loss functions for road extraction form massachusetts dataset.

		F1	MCC	IOU
VNet+CE	Image1	0.9242	0.9103	0.8590
	Image2	0.8825	0.8633	0.7897
	Image3	0.8616	0.8347	0.7568
	Average	0.8894	0.8694	0.8018
VNet+DL	Image1	0.9268	0.9133	0.8635
	Image2	0.8973	0.8801	0.8138
	Image3	0.8705	0.8454	0.7706
	Average	0.8982	0.8796	0.8159
VNet+CEDL	Image1	0.9289	0.9159	0.8672
	Image2	0.9027	0.8865	0.8225
	Image3	0.8717	0.8466	0.7725
	Average	0.9011	0.8830	0.8207

verifying the effectiveness of our approach in road extraction. Furthermore, the suggested VNet+CEDL network could
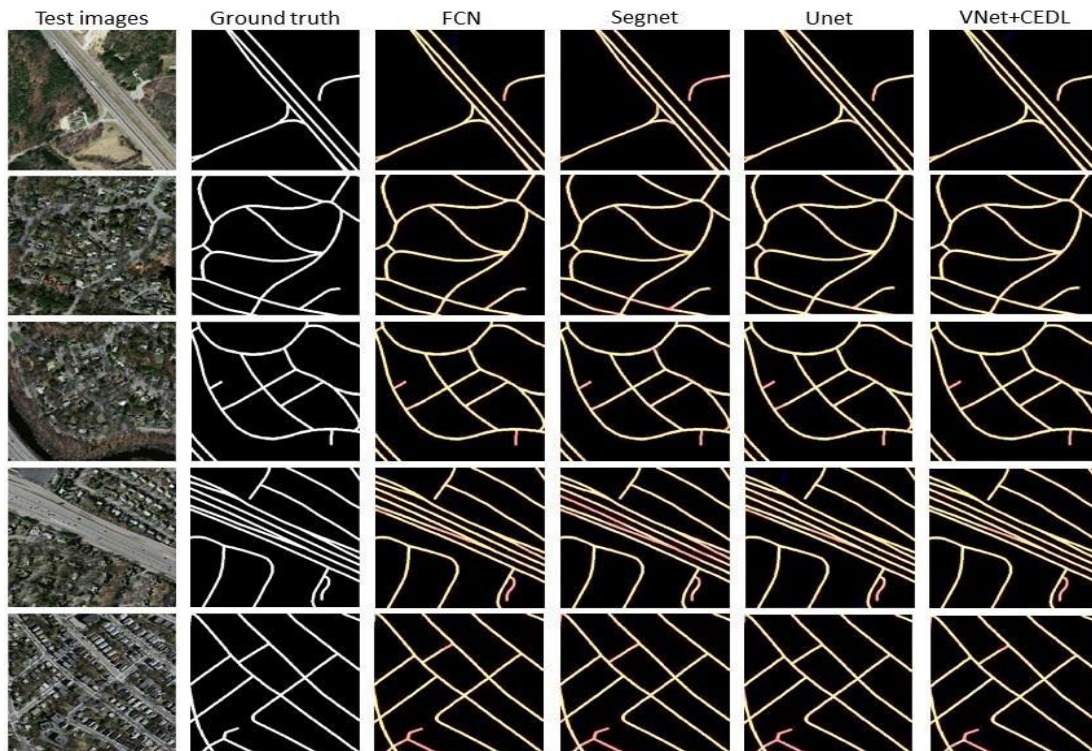
FIGURE 7. Road segmentation results obtained by the proposed VNet+CEDL against other comparison approaches from the Massachusetts road dataset. The yellow, blue, and red colors show the TPs, FPs and FNs, respectively.

FIGURE 8. Road segmentation results obtained by the proposed VNet+CEDL against other comparison approaches from the Ottawa road dataset. The yellow color, blue and red colors depict the TPs, FPs, and FNs, respectively.

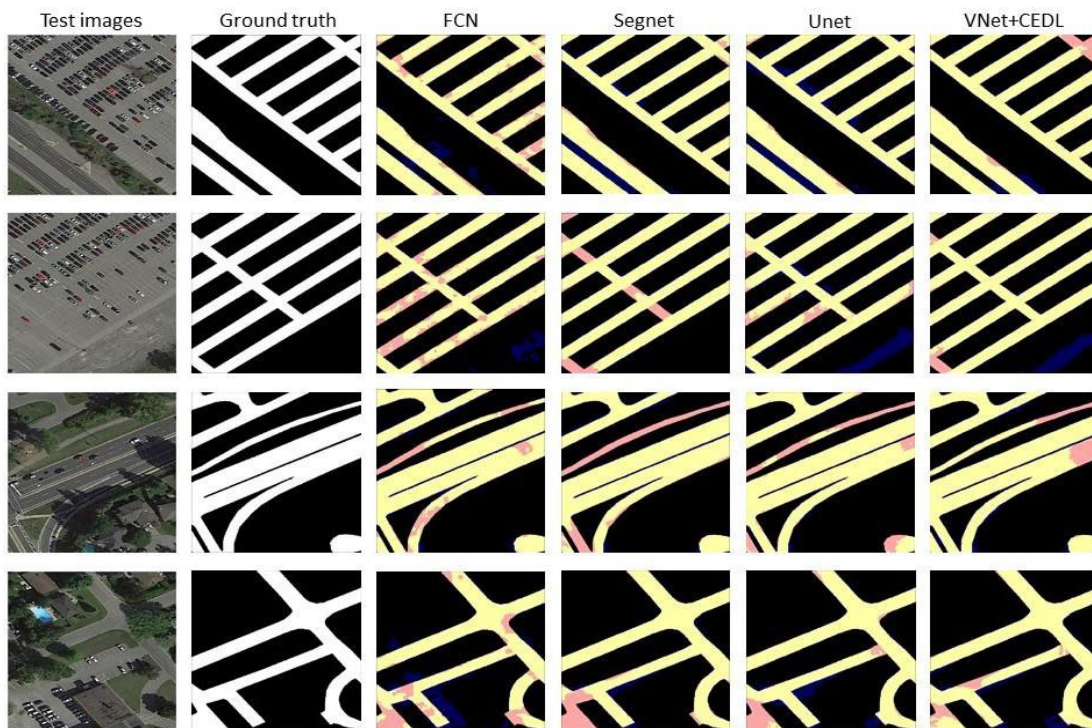maintain edge information and achieve higher precision on the segmentation boundary than the other comparative approaches.

IV. DISCUSSION

The obtained measurement factors in the current work and in other studies were compared to further explore the

TABLE 2. Comparing VNet model with CE, DL and CEDL loss functions for road extraction form ottawa dataset.

		F1	MCC	IOU
Vnet+CE	Image1	0.9361	0.9060	0.8799
	Image2	0.8814	0.8099	0.7878
	Image3	0.9391	0.9030	0.8852
	Average	0.9189	0.8730	0.8510
Vnet+DL	Image1	0.9551	0.9338	0.9141
	Image2	0.9022	0.8437	0.8218
	Image3	0.9416	0.9074	0.8896
	Average	0.9329	0.8949	0.8751
Vnet+CEDL	Image1	0.9563	0.9356	0.9162
	Image2	0.9069	0.8509	0.8295
	Image3	0.9431	0.9102	0.8922
	Average	0.9354	0.8989	0.8793

benefit of the suggested approach for road network extraction from high-resolution remote sensing imagery. For comparison, we used the results achieved by VNet+CEDL for both Massachusetts and Ottawa datasets as it shows better results in road extraction compared to VNet+CE. Particularly, the proposed approach was compared with some deep learning-based neural networks such as Unet framework introduced by [36], FCN proposed by [48] for image semantic segmentation and Segnet architecture applied by [49] for sematic pixel-wise segmentation. The quantitative results achieved by the proposed technique and other comparisons approaches for both Massachusetts and Ottawa road datasets are illustrated in Table 3 and Table 4. By comparing the results achieved for each metric, the difference between the precision for road extraction can be observed. As illustrated in Table 3 and 4, the proposed VNet+CEDL model could achieve higher average accuracy for the whole three evaluation metrics (F1, MCC and IOU) than other cutting-edge deep learning-based techniques for both datasets. In fact, the model predicts less FPs and more FNs than other methods, leading to the improve in the results for IOU factor with almost 0.66%, 3.99% and 1.85% compared to Unet, Segnet and FCN for Massachusetts dataset respectively and 4.38%, 3.09% and 11.17% for Ottawa dataset, respectively.

Moreover, Figure 7 and 8 depict the visual results obtained by the introduced VNet+CEDL model and other state-of-the-art deep learning-based techniques for Massachusetts road dataset and Ottawa dataset, respectively to show the proficiency of the proposed model in road extraction. The results demonstrate that the proposed deep learning-based models could generally reduce the effect of obstacles to a particular degree as they are using spatial information for segmentation. However, the other methods such as Unet, Segnet and FCN could anticipate more FNs than the proposed VNet+CEDL model that could predict less FPs and

TABLE 3. Quantitative outcomes achieved by the Vnet+CEDL and other techniques for massachusetts dataset.

		FCN	Segnet	Unet	VNet_CEDL
Image1	F1	0.9120	0.8916	0.9283	0.9314
	MCC	0.8993	0.8759	0.9180	0.9216
	IOU	0.8381	0.8043	0.8662	0.8716
Image2	F1	0.9058	0.8933	0.9076	0.9087
	MCC	0.8891	0.8742	0.8910	0.8924
	IOU	0.8278	0.8072	0.8308	0.8327
Image3	F1	0.9048	0.9083	0.9087	0.9152
	MCC	0.8887	0.8928	0.8933	0.9008
	IOU	0.8261	0.8320	0.8327	0.8437
Image4	F1	0.8785	0.8392	0.8864	0.8933
	MCC	0.8489	0.8022	0.8588	0.8675
	IOU	0.7832	0.7229	0.7959	0.8072
Image5	F1	0.9032	0.9041	0.9084	0.9105
	MCC	0.8860	0.8874	0.8922	0.8947
	IOU	0.8235	0.8249	0.8322	0.8356
Average	F1	0.9009	0.8873	0.9079	0.9118
	MCC	0.8824	0.8665	0.8907	0.8954
	IOU	0.8197	0.7983	0.8316	0.8382

TABLE 4. Quantitative outcomes achieved by the VNet+CEDL and other techniques for ottawa dataset.

		FCN	Segnet	Unet	VNet+CEDL
Image1	F1	0.8665	0.907	0.8867	0.9236
	MCC	0.799	0.8501	0.8181	0.8793
	IOU	0.7643	0.8297	0.7965	0.858
Image2	F1	0.7886	0.9005	0.8602	0.9093
	MCC	0.7193	0.8538	0.7864	0.8622
	IOU	0.6509	0.8189	0.7547	0.8336
Image3	F1	0.9046	0.887	0.91	0.9178
	MCC	0.8455	0.8202	0.8565	0.8662
	IOU	0.8258	0.797	0.8347	0.848
Image4	F1	0.8034	0.8826	0.8876	0.9009
	MCC	0.7268	0.8388	0.8415	0.8608
	IOU	0.6714	0.7899	0.7979	0.8197
Average	F1	0.8408	0.8943	0.8861	0.9129
	MCC	0.7727	0.8407	0.8256	0.8671
	IOU	0.7281	0.8089	0.7960	0.8398

consequently could achieve better results. This is because this technique could obtain and preserve boundary information that leads to anticipating less FPs and achieving high-resolution and smooth segmentation maps compared to

the other deep learning-based methods. Moreover, we compared the results achieved by the proposed model with more several deep learning-based networks such as CNN [50] and road structure-refined CNN model (RSRCNN) [47] for Massachusetts dataset and CasNet [10] and RoadNet [44] for Ottawa dataset. Note that the outcomes for the other methods were chosen from the main published papers, whereas the suggested approach has been performed and tested on the experimental datasets. The visualization and quantitative results for the proposed network and other comparative methods are shown in Figure 9, Table 5 and Table 6, respectively. In terms of F1, the outcomes illustrate that our suggested technique is superior to all other approaches. Our suggested technique achieves higher F1 accuracy than those of [47] and [50], at 39.69% and 26.69% for Massachusetts and higher F1 precision than those of [10] and [44], at 0.67% and 0.17% for Ottawa dataset, respectively.
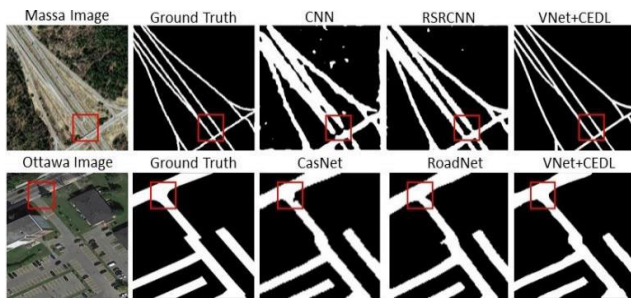

FIGURE 9. Comparison of road segmentation achieved with the suggested approach (VNet+CEDL) against other techniques for Massachusetts and Ottawa datasets.

TABLE 5. Quantitative values on the testing data of massachusetts dataset in terms of F1.

Method	CNN [47]	RSRCNN [50]	VNet+CEDL
F1	0.5320	0.6620	0.9289

TABLE 6. Quantitative values on the testing data of ottawa dataset in terms of F1.

Method	CasNet [10]	RoadNet [44]	VNet+CEDL
F1	0.9340	0.9390	0.9407

V. CONCLUSION

In the present work, we applied a new deep convolutional neural network called VNet model to extract road network from high-resolution remote sensing imagery. Also, we implemented a new loss function named CEDL to decrease the problem of class imbalance in our datasets and improved the result of road segmentation. We utilized two different remote sensing datasets such as Massachusetts and Ottawa road datasets that contained aerial imagery and Google Earth imagery, respectively. Also, we calculated different important

accuracy measurements such as F1, MCC and IOU to evaluate the performance of the suggested technique in road extraction. The proposed VNet+CEDL model could achieve an average F1 accuracy of 91.18% for Massachusetts dataset and 91.29% for Ottawa dataset confirmed that the model could obtain accurate road results and produce high-resolution segmentation map. Moreover, the proposed deep convolutional model is compared with other deep learning-based techniques, and the visual and quantitative outcomes prove the superiority of proposed method in road extraction from high-resolution remote sensing imagery.

AUTHOR CONTRIBUTIONS

Conceptualization, A.A. and B.P.; methodology and formal analysis, A.A.; data curation, A.A.; writing—original draft preparation, A.A.; writing—review and editing, B.P.; supervision, B.P.; funding – B.P. and A.A.A., All authors have read and agreed to the published version of the manuscript.

CONFLICT OF INTEREST

The authors declare no conflict of interest.

REFERENCES

[1] Y. Xu, L. Wu, Z. Xie, and Z. Chen, "Building extraction in very high resolution remote sensing imagery using deep learning and guided filters," *Remote Sens.*, vol. 10, no. 1, p. 144, Jan. 2018.

[2] Q. Weng, "Remote sensing of impervious surfaces in the urban areas: Requirements, methods, and trends," *Remote Sens. Environ.*, vol. 117, pp. 34–49, Feb. 2012.

[3] A. M. Youssef, S. A. Sefry, B. Pradhan, and E. A. Alfadail, "Analysis on causes of flash flood in Jeddah city (Kingdom of saudi Arabia) of 2009 and 2011 using multi-sensor remote sensing data and GIS," *Geomatics, Natural Hazards Risk*, vol. 7, no. 3, pp. 1018–1042, May 2016.

[4] A. Abdollahi, B. Pradhan, and N. Shukla, "Extraction of road features from UAV images using a novel level set segmentation approach," *Int. J. Urban Sci.*, vol. 23, no. 3, pp. 1–15, 2019.

[5] Z. Zhang, Q. Liu, and Y. Wang, "Road extraction by deep residual U-Net," *IEEE Geosci. Remote Sens. Lett.*, vol. 15, no. 5, pp. 749–753, May 2018.

[6] Y. Xu, Z. Xie, Y. Feng, and Z. Chen, "Road extraction from high-resolution remote sensing imagery using deep learning," *Remote Sens.*, vol. 10, no. 9, p. 1461, 2018.

[7] H. R. R. Bakhtiari, A. Abdollahi, and H. Rezaeian, "Semi automatic road extraction from digital images," *Egyptian J. Remote Sens. Space Sci.*, vol. 20, no. 1, pp. 117–123, 2017.

[8] J. Zhang, L. Chen, C. Wang, L. Zhuo, Q. Tian, and X. Liang, "Road recognition from remote sensing imagery using incremental learning," *IEEE Trans. Intell. Transp. Syst.*, vol. 18, no. 11, pp. 2993–3005, Nov. 2017.

[9] J. Wang, J. Song, M. Chen, and Z. Yang, "Road network extraction: A neural-dynamic framework based on deep learning and a finite state machine," *Int. J. Remote Sens.*, vol. 36, no. 12, pp. 3144–3169, Jun. 2015.

[10] G. Cheng, Y. Wang, S. Xu, H. Wang, S. Xiang, and C. Pan, "Automatic road detection and centerline extraction via cascaded end-to-end convolutional neural network," *IEEE Trans. Geosci. Remote Sens.*, vol. 55, no. 6, pp. 3322–3337, Jun. 2017.

[11] A. Abdollahi, B. Pradhan, N. Shukla, S. Chakraborty, and A. Alamri, "Deep learning approaches applied to remote sensing datasets for road extraction: A state-of-the-art review," *Remote Sens.*, vol. 12, no. 9, p. 1444, May 2020.

[12] M. O. Sghaier and R. Lepage, "Road extraction from very high resolution remote sensing optical images based on texture analysis and beamlet transform," *IEEE J. Sel. Topics Appl. Earth Observ. Remote Sens.*, vol. 9, no. 5, pp. 1946–1958, May 2016.

[13] Y. Zhang, Z. Xiong, Y. Zang, C. Wang, J. Li, and X. Li, "Topology-aware road network extraction via multi-supervised generative adversarial networks," *Remote Sens.*, vol. 11, no. 9, p. 1017, Apr. 2019.

[14] J. Cheng, W. Ding, X. Ku, and J. Sun, "Road extraction from high-resolution SAR images via automatic local detecting and human-guided global tracking," *Int. J. Antennas Propag.*, vol. 2012, pp. 1–10, Jan. 2012.

[15] C. Unsalan and B. Sirmacek, "Road network detection using probabilistic and graph theoretical methods," *IEEE Trans. Geosci. Remote Sens.*, vol. 50, no. 11, pp. 4441–4453, Apr. 2012.

[16] E. Khesali, M. J. V. Zoej, M. Mokhtarzade, and M. Dehghani, "Semi automatic road extraction by fusion of high resolution optical and radar images," *J. Indian Soc. Remote Sens.*, vol. 44, no. 1, pp. 21–29, 2016.

[17] Z. Miao, B. Wang, W. Shi, and H. Zhang, "A semi-automatic method for road centerline extraction from VHR images," *IEEE Geosci. Remote Sens. Lett.*, vol. 11, no. 11, pp. 1856–1860, Nov. 2014.

[18] A. Buslaev, S. S. Seferbekov, V. Iglovikov, and A. Shvets, "Fully convolutional network for automatic road extraction from satellite imagery," in *Proc. CVPR Workshops*, 2018, pp. 207–210, doi: 10.1109/CVPRW.2018.00035.

[19] R. Kestur, S. Farooq, R. Abdal, E. Mehraj, O. S. Narasipura, and M. Mudigere, "UFCN: A fully convolutional neural network for road extraction in RGB imagery acquired by remote sensing from an unmanned aerial vehicle," *J. Appl. Remote Sens.*, vol. 12, no. 1, 2018, Art. no. 016020.

[20] S. Tian, X. Zhang, J. Tian, and Q. Sun, "Random forest classification of wetland landcovers from multi-sensor data in the arid region of Xinjiang, China," *Remote Sens.*, vol. 8, no. 11, p. 954, Nov. 2016.

[21] A. Abdollahi, H. R. R. Bakhtiari, and M. P. Nejad, "Investigation of SVM and level set interactive methods for road extraction from Google Earth images," *J. Indian Soc. Remote Sens.*, vol. 46, no. 3, pp. 423–430, Mar. 2018.

[22] Z. Da-Ming, W. Xiang, and L. Chun-Li, "Road extraction based on the algorithms of MRF and hybrid model of SVM and FCM," in *Proc. Int. Symp. Image Data Fusion Image Data Fusion (ISIDF)*, Yunnan, China, 2011, pp. 1–4.

[23] R. M. Anwer, F. S. Khan, J. van de Weijer, M. Molinier, and J. Laaksonen, "Binary patterns encoded convolutional neural networks for texture recognition and remote sensing scene classification," *ISPRS J. Photogramm. Remote Sens.*, vol. 138, pp. 74–85, Apr. 2018.

[24] C. Simler, "An improved road and building detector on VHR images," in *Proc. IEEE Int. Geosci. Remote Sens. Symp.*, Jul. 2011, pp. 507–510.

[25] N. Yager and A. Sowmya, "Support vector machines for road extraction from remotely sensed images," in *Proc. Int. Conf. Comput. Anal. Images Patterns*, 2003, pp. 285–292.

[26] P. Li, Y. Zang, C. Wang, J. Li, M. Cheng, L. Luo, and Y. Yu, "Road network extraction via deep learning and line integral convolution," in *Proc. IEEE Int. Geosci. Remote Sens. Symp. (IGARSS)*, Jul. 2016, pp. 1599–1602.

[27] L. Zhang, F. Yang, Y. Daniel Zhang, and Y. J. Zhu, "Road crack detection using deep convolutional neural network," in *Proc. IEEE Int. Conf. Image Process. (ICIP)*, Sep. 2016, pp. 3708–3712.

[28] F. Zhou, H. Hang, and Q. Liu, "Class-guided feature decoupling network for airborne image segmentation," *IEEE Trans. Geosci. Remote Sens.*, early access, Jul. 15, 2020, doi: 10.1109/TGRS.2020.3006872.

[29] R. Hang, F. Zhou, Q. Liu, and P. Ghamisi, "Classification of hyperspectral images via multitask generative adversarial networks," *IEEE Trans. Geosci. Remote Sens.*, early access, Jun. 25, 2020, doi: 10.1109/TGRS.2020.3003341.

[30] D. Hong, L. Gao, N. Yokoya, J. Yao, J. Chanussot, Q. Du, and B. Zhang, "More diverse means better: Multimodal deep learning meets remote-sensing imagery classification," *IEEE Trans. Geosci. Remote Sens.*, early access, Aug. 24, 2020, doi: 10.1109/TGRS.2020.3016820.

[31] P. Li, Y. Zang, C. Wang, J. Li, M. Cheng, L. Luo, and Y. Yu, "Road network extraction via deep learning and line integral convolution," in *Proc. IEEE Int. Geosci. Remote Sens. Symp. (IGARSS)*, Beijing, China, Jul. 2016, pp. 1599–1602, doi: 10.1109/IGARSS.2016.7729406.

[32] T. Panboonyuen, K. Jitkajornwanich, S. Lawawirojwong, P. Srestasathiern, and P. Vateekul, "Road segmentation of remotely-sensed images using deep convolutional neural networks with landscape metrics and conditional random fields," *Remote Sens.*, vol. 9, no. 7, p. 680, Jul. 2017.

[33] T. Panboonyuen, P. Vateekul, K. Jitkajornwanich, and S. Lawawirojwong, "An enhanced deep convolutional encoder-decoder network for road segmentation on aerial imagery," in *Proc. Int. Conf. Comput. Inf. Technol.* Cham, Switzerland: Springer, 2017, pp. 191–201, doi: 10.1007/978-3-319-60663-7_18.

[34] N. Varia, A. Dokania, and J. Senthilnath, "DeepExt: A convolution neural network for road extraction using RGB images captured by UAV," in *Proc. IEEE Symp. Ser. Comput. Intell. (SSCI)*, Bangalore, India, Nov. 2018, pp. 1890–1895, doi: 10.1109/SSCI.2018.8627717.

[35] Y. Xu, Y. Feng, Z. Xie, A. Hu, and X. Zhang, "A research on extracting road network from high resolution remote sensing imagery," in *Proc. 26th Int. Conf. Geoinformat.*, Kunming, China, 2018, pp. 1–4, doi: 10.1109/GEOINFORMATICS.2018.8557042.

[36] O. Ronneberger, P. Fischer, and T. Brox, "U-net: Convolutional networks for biomedical image segmentation," in *Proc. Int. Conf. Med. Image Comput.-Assist. Intervent*, 2015, pp. 234–241.

[37] K. He, X. Zhang, S. Ren, and J. Sun, "Deep residual learning for image recognition," in *Proc. IEEE Conf. Comput. Vis. Pattern Recognit.*, Jun. 2016, pp. 770–778.

[38] J. T. Springenberg, A. Dosovitskiy, T. Brox, and M. Riedmiller, "Striving for simplicity: The all convolutional net," pp. 1–14, 2014, *arXiv:1412.6806*. [Online]. Available: https://arxiv.org/abs/1412.6806

[39] M. D. Zeiler and R. Fergus, "Visualizing and understanding convolutional networks," in *Proc. Eur. Conf. Comput. Vis.*, 2014, pp. 818–833.

[40] K. He, X. Zhang, S. Ren, and J. Sun, "Delving deep into rectifiers: Surpassing human-level performance on ImageNet classification," in *Proc. IEEE Int. Conf. Comput. Vis.*, Dec. 2015, pp. 1026–1034.

[41] Y. S. Aurelio, G. M. de Almeida, C. L. de Castro, and A. P. Braga, "Learning from imbalanced data sets with weighted cross-entropy function," *Neural Process. Lett.*, vol. 50, no. 2, pp. 1937–1949, Oct. 2019.

[42] X. Li, X. Sun, Y. Meng, J. Liang, F. Wu, and J. Li, "Dice loss for data-imbalanced NLP tasks," pp. 1–13, 2019, *arXiv:1911.02855*. [Online]. Available: http://arxiv.org/abs/1911.02855

[43] V. Mnih, "Machine learning for aerial image labeling," Ph.D. dissertation, Dept. Comput. Sci., Univ. Toronto, Toronto, ON, Canada, 2013.

[44] Y. Liu, J. Yao, X. Lu, M. Xia, X. Wang, and Y. Liu, "RoadNet: Learning to comprehensively analyze road networks in complex urban scenes from high-resolution remotely sensed images," *IEEE Trans. Geosci. Remote Sens.*, vol. 57, no. 4, pp. 2043–2056, Apr. 2019.

[45] C. Poullis, "Tensor-cuts: A simultaneous multi-type feature extractor and classifier and its application to road extraction from satellite images," *ISPRS J. Photogramm. Remote Sens.*, vol. 95, pp. 93–108, Sep. 2014.

[46] N. Ghasemkhani, S. S. Vayghan, A. Abdollahi, B. Pradhan, and A. Alamri, "Urban development modeling using integrated fuzzy systems, ordered weighted averaging (OWA), and geospatial techniques," *Sustainability*, vol. 12, no. 3, p. 809, Jan. 2020.

[47] Y. Wei, Z. Wang, and M. Xu, "Road structure refined CNN for road extraction in aerial image," *IEEE Geosci. Remote Sens. Lett.*, vol. 14, no. 5, pp. 709–713, May 2017.

[48] J. Long, E. Shelhamer, and T. Darrell, "Fully convolutional networks for semantic segmentation," in *Proc. IEEE Conf. Comput. Vis. Pattern Recognit.*, Jun. 2015, vol. 39, no. 4, pp. 3431–3440.

[49] V. Badrinarayanan, A. Kendall, and R. Cipolla, "SegNet: A deep convolutional encoder-decoder architecture for image segmentation," *IEEE Trans. Pattern Anal. Mach. Intell.*, vol. 39, no. 12, pp. 2481–2495, Dec. 2017.

[50] Z. Zhong, J. Li, W. Cui, and H. Jiang, "Fully convolutional networks for building and road extraction: Preliminary results," in *Proc. IEEE Int. Geosci. Remote Sens. Symp. (IGARSS)*, Beijing, China, Jul. 2016, pp. 1591–1594, doi: 10.1109/IGARSS.2016.7729406.

ABOLFAZL ABDOLLAHI received the B.Sc. degree from the Ferdowsi University of Mashhad, Iran, and the M.Sc. degree in GIS and remote sensing from the Kharazmi University of Tehran, Iran. He is currently pursuing the Ph.D. degree with the Centre for Advanced Modelling and Geospatial Information Systems (CAMGIS), University of Technology Sydney (UTS). His research interests include application of advance machine learning approaches and deep learning-based networks for remote sensing image classification, image segmentation, feature extraction, and GIS maps database updating. He was rewarded the International Research Scholarship and the UTS Presidents' Scholarship for the current course in 2018. He has published numerous peer-reviewed articles on the application of machine learning approaches.

BISWAJEET PRADHAN (Senior Member, IEEE) received the Habilitation degree in remote sensing from the Dresden University of Technology, Germany, in 2011. He is currently the Director of the Centre for Advanced Modelling and Geospatial Information Systems (CAMGIS), Faculty of Engineering and IT. He is also the Distinguished Professor with the University of Technology Sydney. He is also an internationally established Scientist in the fields of geospatial information systems (GIS), remote sensing and image processing, complex modeling/geo-computing, machine learning and soft-computing applications, natural hazards, and environmental modeling. Since 2015, he has been serving as the Ambassador Scientist for the Alexander Humboldt Foundation, Germany. Out of his more than 550 articles, more than 500 have been published in science citation index (SCI/SCIE) technical journals. He has authored eight books and 13 book chapters. He was a recipient of the Alexander von Humboldt Fellowship from Germany. He received 55 awards in recognition of his excellence in teaching, service, and research, since 2006. He was also a recipient of the Alexander von Humboldt Research Fellowship from Germany. From 2016 to 2019, he was listed as the World's Most Highly Cited Researcher by Clarivate Analytics Report as one of the world's most influential mind. From 2018 to 2020, he was awarded as the World Class Professor by the Ministry of Research, Technology, and Higher Education, Indonesia. He is also an Associate Editor and an Editorial Member of more than eight ISI journals. He has widely travelled abroad, visiting more than 52 countries to present his research findings.

ABDULLAH ALAMRI received the B.S. degree in geology from King Saud University (KSU), in 1981, the M.Sc. degree in applied geophysics from the University of South Florida, Tampa, in 1985, and the Ph.D. degree in earthquake seismology from the University of Minnesota, USA, in 1990. He is currently a Professor of earthquake seismology and the Director of the Seismic Studies Center, KSU. He is also the President of the Saudi Society of Geosciences. His research interests include crustal structures and seismic micro zoning of the Arabian Peninsula. His recent projects involve also applications of EM and MT in deep groundwater exploration of Empty Quarter and geothermal prospecting of volcanic Harrats in the Arabian shield. He has published more than 150 research articles, achieved more than 45 research projects, as well as authored several books and technical reports. He is a member of the Seismological Society of America, the American Geophysical Union, the European Association for Environmental and Engineering Geophysics, Earthquakes Mitigation in the Eastern Mediterranean Region, the National Committee for Assessment and Mitigation of Earthquake Hazards in Saudi Arabia, and Mitigation of Natural Hazards Com at Civil Defense. He is a Principal and a Co-Investigator in several national and international projects (KSU, KACST, NPST, IRIS, CTBTO, US Air force, NSF, UCSD, LLNL, OSU, PSU, and Max Planck). He obtained several worldwide prizes and awards for his scientific excellence and innovation. He has also chaired and co-chaired several SSG, GSF, RELEMR workshops and forums in the Middle East. He is also the Editor-in-Chief of the *Arabian Journal of Geosciences* (AJGS).

● ● ●